Journal of Fluorescence (2021) 31:1211–1218
https://doi.org/10.1007/s10895-021-02725-0

ORIGINAL ARTICLE

A Rhodamine-based Fluorescent Chemodosimeter for Au^{3+} in Aqueous Solution and Living Cells

Chariwat Pitsanuwong[1] · Juthamanee Boonwan[1] · Sinchai Chomngam[2,3] · Kanokorn Wechakorn[4] · Phongthon Kanjanasirirat[5] · Yongyut Pewkliang[5] · Supareerk Borwornpinyo[5,6] · Palangpon Kongsaeree[2,3]

Received: 28 August 2020 / Accepted: 17 March 2021 / Published online: 27 May 2021

Abstract

A highly selective rhodamine hydrazide-based fluorescent chemosensor for Au^{3+} detection was developed. The aqueous solution of rhodamine *N*-hydroxysemicarbazide (**RHS**), in the presence of Au^{3+}, exhibited a significant 55-fold turn-on fluorescence response at 591 nm and a colorimetric change from colorless to pink. Other interested ions including Li^+, Na^+, K^+, Cs^+, Mg^{2+}, Ca^{2+}, Ba^{2+}, Pb^{2+}, Mn^{2+}, Co^{2+}, Ni^{2+}, Ag^+, Cd^{2+}, Cu^{2+}, Hg^{2+}, Zn^{2+}, Sn^{2+}, Fe^{2+}, Fe^{3+}, Cr^{3+}, Ce^{3+} did not induce any distinct color/spectral changes. The irreversible detection mechanism occurred via Au^{3+}-promoted 5-*exo-trig* ring closure to yield 1,3,4-oxadiazole-2-one product. The **RHS** probe is non-responsive to other biologically relevant metal ions and the limit of detection for Au^{3+} was calculated to be 0.5 μM with a linear range of 0 to 90 μM. Fluorescence bioimaging of Au^{3+} in HepG2 cells was also successfully demonstrated.

Keywords Au^{3+}-selective chemosensor · *N*-hydroxysemicarbazide · Rhodamine · Fluorescence detection · Bioimaging

Introduction

Gold has attracted a great deal of scientific attention due to their potential in catalysis and biomedical applications [1–4]. The characteristic alkynophilicity of gold ions leads to a series of chemical transformations to construct complex molecular structures [5–8]. Gold-based compounds are also beneficial for the treatment of various diseases including rheumatic arthritis, tuberculosis, asthma, malaria, cancer, brain lesions and HIV [9–11]. Gold nanoparticles have been applied for drug delivery into cells and for sensors in biological processes [12–15]. Nonetheless, gold salts can damage liver, kidneys, and peripheral nervous system. Strong affinity of Au^{3+} to enzyme and DNA could lead to DNA damage by a catalytic cleavage [16, 17]. Therefore, it is highly attractive to develop efficient methods to detect gold species in both biological and environmental settings. The traditional analytical methods have been used to detect gold ions including electrochemistry, atomic absorption and ICP mass spectrometry [18]. Because of these typical methods are unsuitable for detecting biological samples, sensitive and efficient fluorescent chemosensors are useful for monitoring biologically relevant species. Fluorescent chemosensors for Au^{3+} have been reported with rhodamine, naphthalimide, rhodol, fluorescein, BODIPY and calixarene as reporter units [19–23]. Several Au^{3+}-selective fluorescent probes were designed based on the alkynophilicity of gold ions [24–31]. For example, Au^{3+} reacted with a propargyl rhodamine conjugate, followed by intramolecular cyclization to form an oxazolecarbaldehyde moiety, resulting in a turn-on fluorescence emission of the rhodamine probe [32].

✉ Chariwat Pitsanuwong
chariwat.ph@ssru.ac.th

✉ Palangpon Kongsaeree
palangpon.kon@mahidol.ac.th

[1] Department of Chemistry, Faculty of Science and Technology, Suan Sunandha Rajabhat University, Bangkok 10400, Thailand

[2] Department of Chemistry, Center of Excellence for Innovation in Chemistry, Faculty of Science, Mahidol University, 10400 Bangkok, Thailand

[3] Center for Excellence in Protein and Enzyme Technology, Faculty of Science, Mahidol University, 10400 Bangkok, Thailand

[4] Department of Chemistry, Faculty of Science and Technology, Rajamangala University of Technology Thanyaburi, 12110 Pathumthani, Thailand

[5] Excellent Center for Drug Discovery, Faculty of Science, Mahidol University, 10400 Bangkok, Thailand

[6] Department of Biotechnology, Faculty of Science, Mahidol University, 10400 Bangkok, Thailand

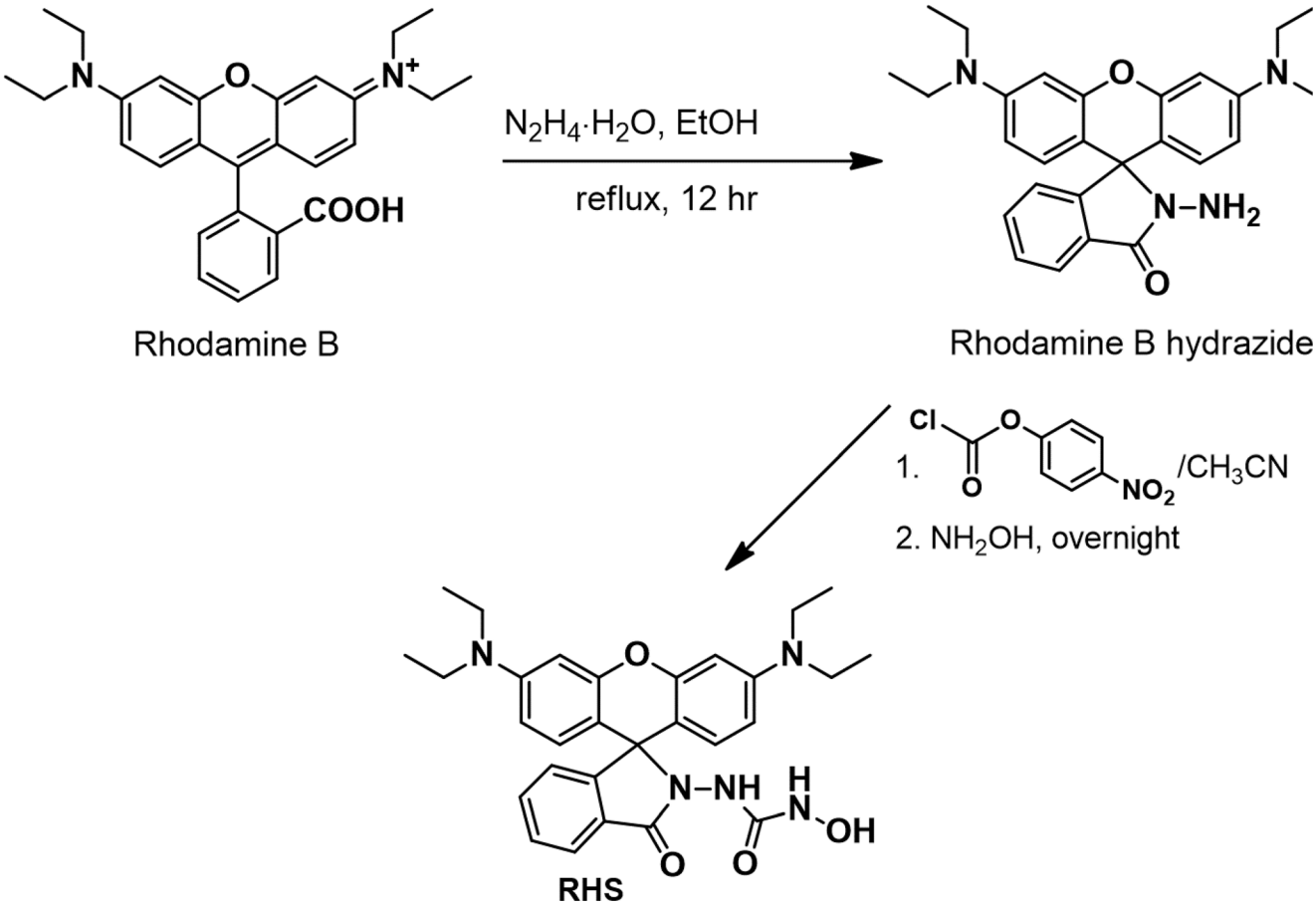

Scheme 1 The synthesis of **RHS** probe

Noteworthy, for rhodamine hydrazides, different alkyl substituents in *N*-alkyl semicarbazide analogs, possessed different specificity toward metal ions including Cu^{2+} and Hg^{2+} [33–38]. Herein, we report a rhodamine hydrazide appended with *N*-hydroxysemicarbazide **RHS** as a highly selective turn-on fluorescent chemodosimeter for Au^{3+} but not Cu^{2+} or Hg^{2+}. **RHS** reacted with Au^{3+} and underwent a cyclization reaction to give a fluorescent product.

The Experimental Section

Chemicals and Instrumentations

All chemicals used in this study were obtained from commercial suppliers and used without further purification. Common solvents including hexane, CH_2Cl_2, EtOAc, MeOH, and acetone were distilled prior to use. Sodium phosphate buffer (10 mM, pH 7.4) was prepared from $Na_2HPO_4{\cdot}12H_2O$ and $NaH_2PO_4{\cdot}2H_2O$. Column chromatographic purification was performed on silica gel 60 (70–230 mesh, Merck). UV-Vis absorption spectra were recorded on an Agilent 89090A spectrophotometer with a 10-mm quartz cuvette. Fluorescence spectra were measured on an Agilent Cary Eclipse fluorescence spectrophotometer. ^{1}H Nuclear magnetic resonance (NMR) and ^{13}C NMR spectra were obtained from a Bruker AV-400 spectrometer in $CDCl_3$ with tetramethylsilane (TMS) as an internal standard. High-resolution electrospray ionization (ESI) mass spectrometric data were measured a Bruker MicrOTOF mass spectrometer. Cell imaging experiments were carried out on an Operetta high-content imaging system (PerkinElmer).

Preparation and Characterization of Rhodamine N-hydroxysemicarbazide

Rhodamine B hydrazide was prepared by using the modified method [39]. Rhodamine (1.92 g, 4.0 mmol) was dissolved in EtOH (40 mL) and hydrazine hydrate (640 μL, 3.3 equiv.) was added dropwise. The reaction mixture was refluxed for 12 h under argon atmosphere. The reaction was monitored by silica gel TLC. The solvent was removed under reduced pressure, extracted with EtOAc (3 · 100 mL), dried over anhydrous $MgSO_4$, and the solvent was removed under reduced

pressure. After recrystallized from EtOH, rhodamine hydrazide was obtained in 76.7 % yield (1.39 g).

The synthesis of the **RHS** probe was carried out using rhodamine hydrazide, 4-nitrobenzoyl chloride and hydroxylamine (Scheme 1). Rhodamine hydrazide (456 mg, 1.0 mmol) was dissolved in MeCN (30 mL) and 4-nitrobenzoyl chloride (241 mg, 1.2 equiv.) was added to the solution and subsequently with hydroxylamine (210 μL, 1.2 equiv.) at room temperature. After 24 h, the solvent was removed under reduced pressure and the crude mixture was purified by silica gel column chromatography (EtOAc as an eluent) to give **RHS** as a pale magenta solid in 35 %yield (180.6 mg). ^{1} H NMR (400 MHz, $CDCl_3$) δ (ppm): 7.8 (d, J = 7.0 Hz, 1 H), 7.4–7.6 (m, 2 H), 6.9–7.2 (d, J = 7.5 Hz, 1 H), 6.6 (d, J = 9.0 Hz, 2 H), 6.4 (s, 2 H), 6.3 (dd, J = 8.9, 2.6 Hz, 2 H), 3.3 (q, J = 7.2 Hz, 8 H), 1.25 (t, J = 7.0 Hz, 12 H). ^{13} C NMR (100 MHz, $CDCl_3$) δ (ppm): 166.5, 159.3, 153.9, 152.2, 149.2, 133.8, 129.4, 128.8, 128.4, 124.3, 123.7, 108.1, 104.0, 98.0, 66.9, 44.5, 12.8. HRMS (ESI) *m/z* calcd. for $C_{29}H_{34}N_5O_4$ $[M+H]^+$: 516.2605, found 516.2584.

General Procedure for Spectroscopic Studies

RHS was dissolved in aqueous EtOH (1:1 *v/v*, 10 mM phosphate buffer, pH 7.4) to provide the test solution (10 μM). All stock solutions (10 mM) of metal cations (Li^+, Na^+, K^+, Cs^+, Mg^{2+}, Ca^{2+}, Ba^{2+}, Pb^{2+}, Mn^{2+}, Co^{2+}, Ni^{2+}, Ag^+, Cd^{2+}, Cu^{2+}, Hg^{2+}, Zn^{2+}, Sn^{2+}, Fe^{2+}, Fe^{3+}, Cr^{3+}, Ce^{3+}, and Au^{3+}) were prepared in 10 mM phosphate buffer, pH 7.4. All measurements were carried out in aqueous EtOH (1:1 *v/v*, 10 mM phosphate buffer, pH 7.4) at room temperature. The samples were excited at 535 nm and the emission spectrum was scanned from 545 nm to 745 nm.

Determination of the Binding Stoichiometry and the Quantum Yield

The binding stoichiometry of **RHS** and Au^{3+} was established by a Job plot. The fluorescence intensity data were plotted against the mole fractions of Au^{3+}. The total concentration of **RHS** and Au^{3+} was kept constant at 10.0 μM. The stock solution of **RHS** (1 mM) and stock solution of Au^{3+} (10 mM) were prepared in EtOH-phosphate buffer (1:1 *v/v*, 10 mM, pH 7.4). Dilutions of the **RHS** (1 equiv.) and Au^{3+} (10 equiv.) solutions were prepared in various **RHS** concentrations in the range of 0.1–0.6 mM. The fluorescence intensity data for each concentration were plotted against the absorbance then the linear fitting of the positive slope was calculated. The fluorescence quantum yield (Φ_F) was evaluated by using rhodamine B as a standard in the range of 5–50 μM EtOH-phosphate buffer (1:1 *v/v*, 10 mM, pH 7.4). The quantum yield of

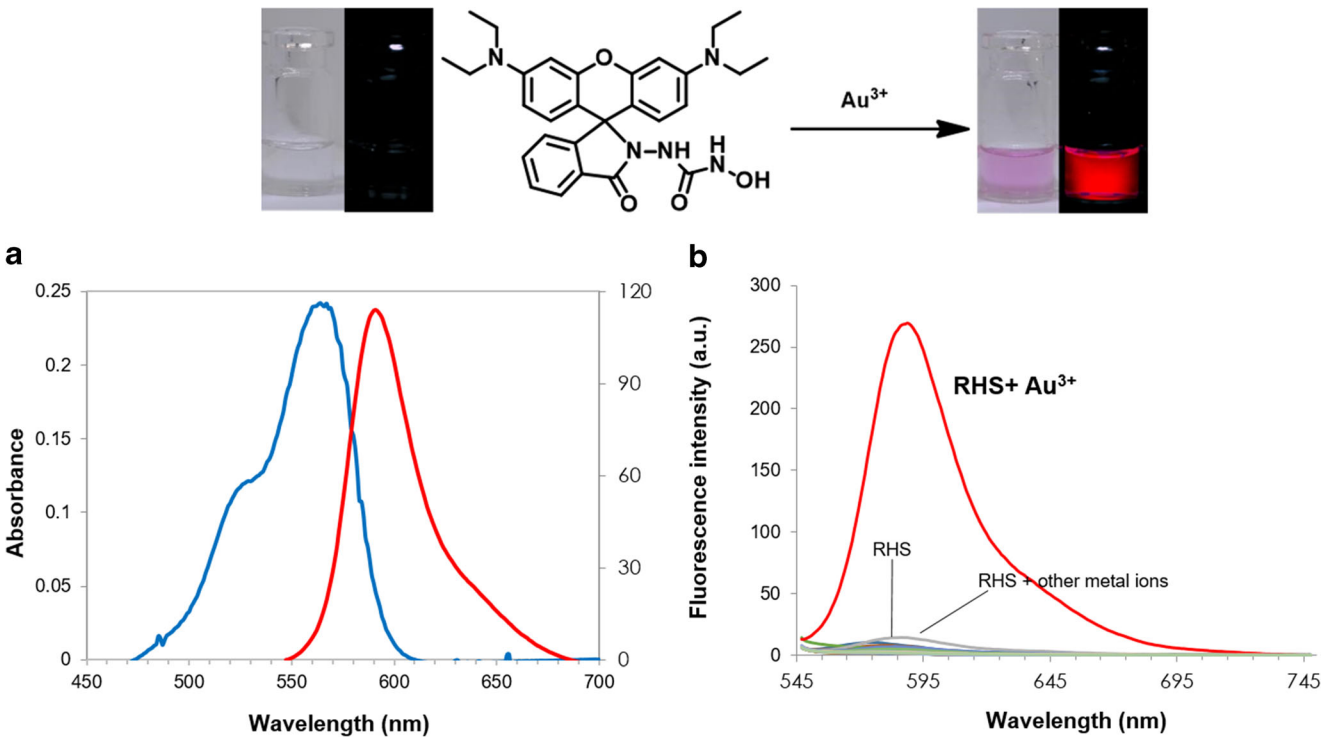

Fig. 1 Chromogenic and fluorogenic response of the **RHS** solution with Au^{3+} (above). (**a**) Absorption and fluorescence spectra of **RHS** (10 μM) with Au^{3+} (1 equiv.) in aqueous EtOH (1:1 *v/v*, 10 mM phosphate buffer, pH 7.4) (**b**) fluorescence responses of **RHS** (10 μM) to Au^{3+} and other interested metal ions (10 equiv.)

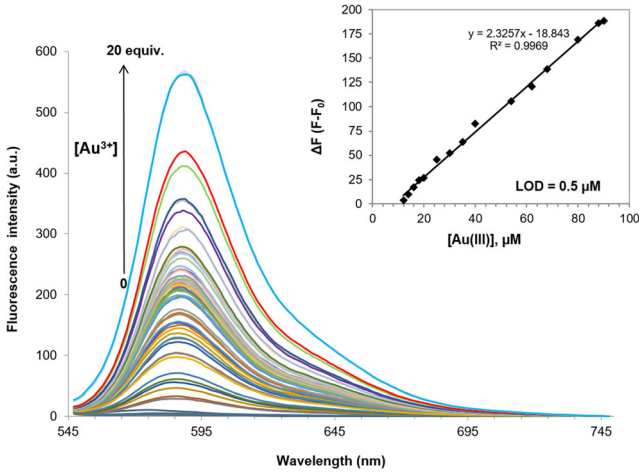

Fig. 2 Fluorescence titration of **RHS** (10 μM) and Au^{3+} (0–20 equiv.) in in aqueous EtOH (1:1 *v/v*, 10 mM phosphate buffer, pH 7.4). Inset; changes of emission intensity at 591 nm (λ_{ex} = 535 nm)

RHS was determined according to the following equation:

$$\Phi_X = \Phi_{ST} \cdot \frac{Grad_X}{Grad_{ST}} \cdot \frac{\eta_X^2}{\eta_{ST}^2}$$

where the subscripts *ST* and *X* denote standard and sample, respectively. Φ is the quantum yield. *Grad* is the slope from the plot of integrated fluorescence intensity and absorbance, and η is the refractive index of the solvent.

Cell Culture and Fluorescence Imaging

HepG2 cells were grown in Dulbecco's modified Eagle's medium (DMEM) with 10 % fetal bovine serum (FBS), 100 μg/ml streptomycin and 100 U/ml penicillin at 37 °C in 5 % CO_2 atmosphere. The cells (3×10^4 cells well) were seeded on sterile glass coverslips in a 96-well plate in culture medium. After 24 h, the cells were treated with $HAuCl_4$ (200 μM) in DMEM at 37 °C for 1 h. Subsequently, the treated cells were washed with the culture medium to remove excess Au^{3+} prior to incubation with **RHS** (20 μM) for 1 h, followed by Hoechst 33342 (20 μM) as a nuclear staining dye. Cells were imaged in DMEM culture medium at 37 °C under 5 % CO_2 with an Operetta high-content imaging system (PerkinElmer) using a 40× objective lens and the Harmony® software. For the fluorescence bioimaging of **RHS**, the emission wavelength was collected a 560–630 nm and the excitation wavelength was set at 520–550 nm. For Hoechst-stained nuclei, the emission wavelength was collected at 410–480 nm and the excitation wavelength was set at 360–400 nm.

Microculture Tetrazolium (MTT) Cell Viability Assays

HepG2 cells (1×10^4 cells/well) were incubated with 0–40 μM **RHS** for 24 h in modified Eagle's medium at 37 °C under humidified 5 % CO_2 atmosphere. Subsequently, the cells were incubated with 0.5 mg/ml MTT (3-(4,5-dimethylthiazol-2-yl)-2,5-diphenyltetrazolium bromide) for 4 h at 37 °C under humidified 5 % CO_2 in an air incubator, followed by adding 100 % DMSO (100 μL) to solubilize the crystals before measurement of absorbance at 570 nm by an EnVision multilabel plate reader (PerkinElmer, Germany). Error bars denote standard error of the mean (SEM), $n = 3$. Hep-G2 cells maintained the cell viability in the presence of **RHS**, revealed by standard MTT assays. Data are reported as percentages of the negative control (Fig. S13).

Results and Discussion

Synthesis of the Prob RHS

The **RHS** chemical probe was prepared in a moderate yield from rhodamine hydrazide, hydroxylamine and 4-

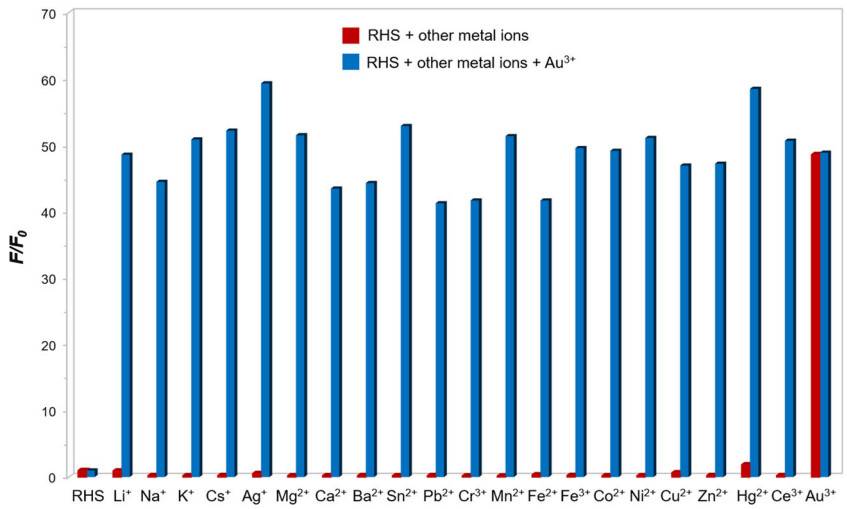

Fig. 3 Fluorescence changes (F/F_0) of **RHS** in various metal ions (3 equiv., red), and in the presence of Au^{3+} (3 equiv., blue) (1:1 *v/v*, EtOH-phosphate buffer, 10 mM, pH 7.4, λ_{ex} = 535 nm, λ_{em} = 591 nm)

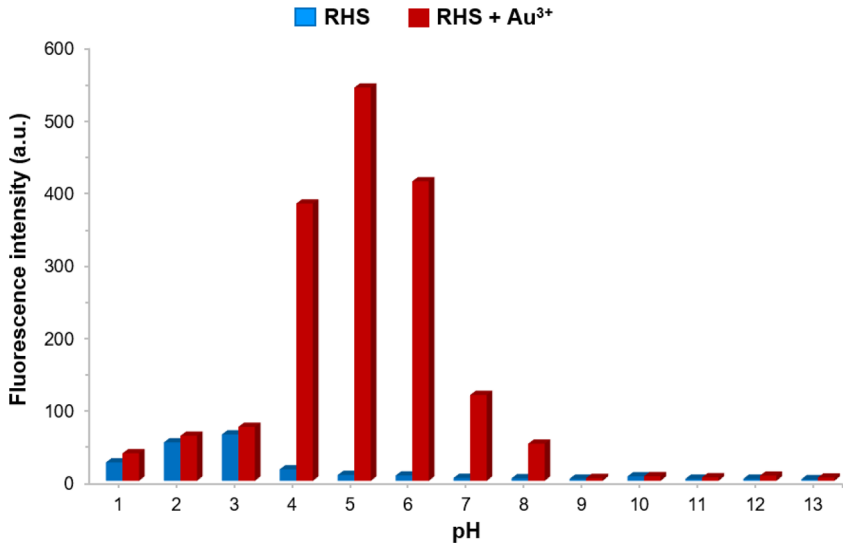

Fig. 4 Fluorescence intensity of **RHS** (10 μM, blue) and in the presence of Au^{3+} (10 equiv., red) in different pH values (λ_{em} = 591 nm)

nitrobenzoyl chloride as shown in Scheme 1. The structure of **RHS** was spectroscopically established by ^{1}H NMR, ^{13}C NMR and ESI-HRMS data (Fig. S1-S3). The characteristic peak of the spirolactam carbon of **RHS** appeared at δ 66.9 ppm in the ^{13}C NMR spectra indicating the closed spirolactam ring [33].

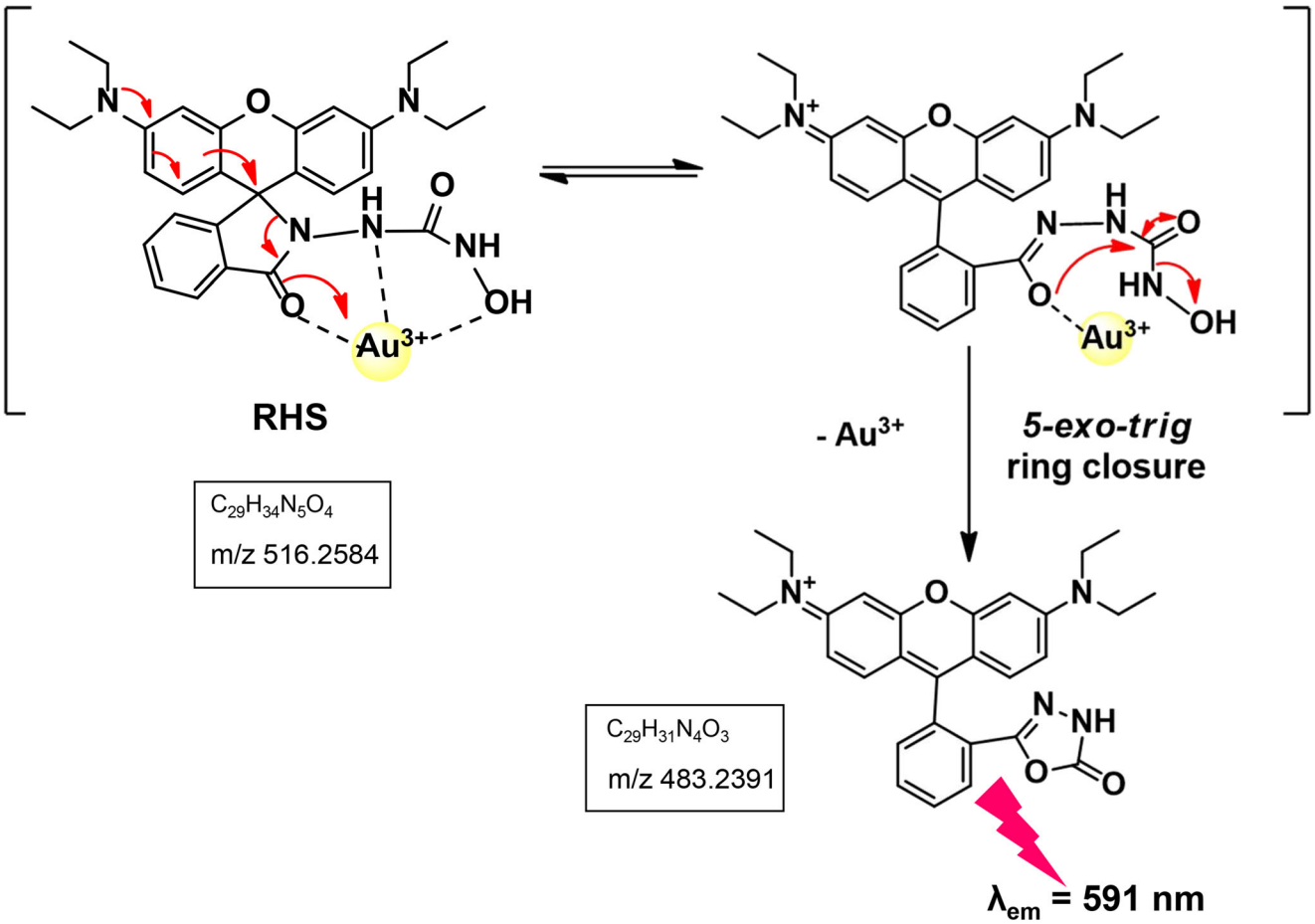

Scheme 2 The proposed sensing mechanism of **RHS** induced by Au^{3+} in aqueous EtOH (1:1 *v*/*v*, 10 mM phosphate buffer, pH 7.4) to yield 1,3,4-oxadiazole-2-one product (λ_{em} = 591 nm)

Photophysical Property and Selectivity of RHS

The solution of **RHS** displayed almost no fluorescence in aqueous EtOH (1:1 *v/v*, 10 mM phosphate buffer, pH 7.4). Preliminarily, the probe solutions were tested with various metal ions and the colorless **RHS** solution changed to pink only in the presence of Au^{3+}. UV-Vis spectral data of the colorless **RHS** solution had no absorption band in the visible region (400–700 nm), indicating the structure existed predominantly in the spirolactam form.

Upon the addition of Au^{3+}, the colorless solution of **RHS** displayed a new absorption spectrum centered at 564 nm. Its fluorescence spectrum revealed a maximum emission band at 591 nm (Fig. 1a) with a 55-fold increase ($\Phi = 0.50$). These data indicated that Au^{3+} promoted the ring opening of the spirolactam unit. To investigate the selectivity of the chemical probe, the fluorescence responses of **RHS** toward other metal ions, including Li^+, Na^+, K^+, Cs^+, Mg^{2+}, Ca^{2+}, Ba^{2+}, Pb^{2+}, Mn^{2+}, Co^{2+}, Ni^{2+}, Ag^+, Cd^{2+}, Cu^{2+}, Hg^{2+}, Zn^{2+}, Sn^{2+}, Fe^{2+}, Fe^{3+}, Cr^{3+}, Ce^{3+}, and Au^{3+}, were recorded in EtOH-phosphate buffer (1:1 *v/v*, 10 mM, pH 7.4) (Fig. 1b and S9). The fluorescence emission, due to the ring-opening reaction of the spirocyclic moiety of **RHS**, was clearly observed only in the presence of Au^{3+}, but not with Cu^{2+} or Hg^{2+} like in previously reported *N*-alkylsemicarbazide rhodamine derivatives [33–37]. These results supported that **RHS** can serve as a highly selective fluorescent probe for Au^{3+} detection. In the fluorescence titration of **RHS** and Au^{3+} (0–20 equiv.) in aqueous EtOH (1:1 *v/v*, 10 mM phosphate buffer, pH 7.4), the fluorescence of **RHS** was linearly enhanced with Au^{3+} concentrations in a range of 0–90 μM (Fig. 2). The limit of detection (LOD) of **RHS** for Au^{3+} was calculated to be 0.5 μM (98 ppb) ($\sigma/N = 3$). In addition, the binding stoichiometry of **RHS** and Au^{3+} was found to be 1:1 based on a Job plot analysis with the maximum fluorescence intensity at the mole fraction of 0.5 (Fig. S10). For a competitive experiment, other metal ions, including Li^+, Na^+, K^+, Cs^+, Mg^{2+}, Ca^{2+}, Ba^{2+}, Pb^{2+}, Mn^{2+}, Co^{2+}, Ni^{2+}, Ag^+, Cd^{2+}, Cu^{2+}, Hg^{2+}, Zn^{2+}, Sn^{2+}, Fe^{2+}, Fe^{3+}, Cr^{3+}, and Ce^{3+}, did not affect the sensing of **RHS** to Au^{3+} (Fig. 3).

The effect of pH values in fluorescence sensing of **RHS** and the **RHS**-Au^{3+} was investigated in a pH range from 1 to 13 (Fig. 4). Without Au^{3+}, **RHS** did not give a clear fluorescence enhancement except in pH 1–3, and with Au^{3+}, enhanced emission was strongly observed in a pH range of 4–7, rendering its possibility to apply **RHS** to monitor Au^{3+} under physiological conditions. Upon the addition of Au^{3+}, a time-course study of the fluorescence enhancement of **RHS** showed the reaction was completed within 12 min (Fig. S11).

Response Mechanism

The signaling mechanism of **RHS** for Au^{3+} was investigated by mixing **RHS** (50 mM) with Au^{3+} (1 equiv.) in aqueous EtOH [32]. In silica gel TLC analysis, upon the disappearance of the **RHS** probe, a less polar spot was observed (Fig. S8). The product was subsequently purified by silica gel PLC and characterized by ^{1}H NMR and ^{13}C NMR and ESI-HRMS analysis (Fig. S4-S7). The MS data displayed an intense peak at *m/z* 483.2401, suggesting the cyclized 1,3,4-oxadiazole-2-one rhodamine derivative (calcd. 483.2391 for $C_{29}H_{31}N_4O_3$). The ^{13}C NMR data revealed two new signals at δ 166.1 and 157.4 ppm, corresponding to the two carbon atoms of the oxadiazolone [40–43]. A

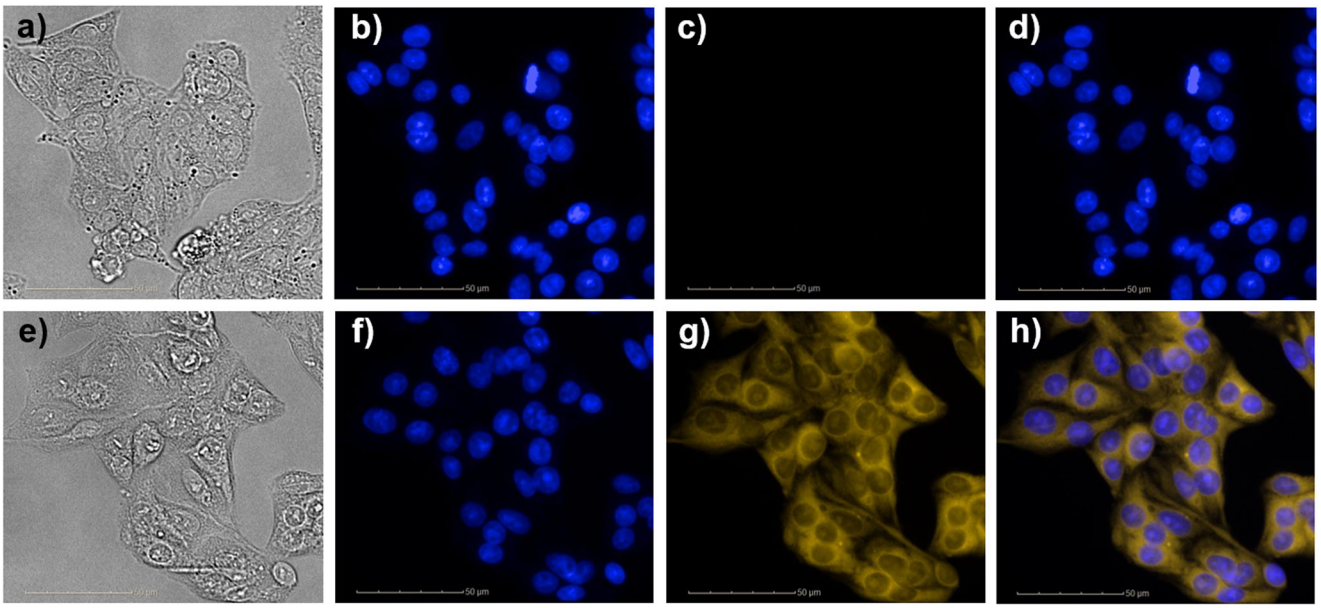

Fig. 5 Confocal fluorescence images of **RHS** in HepG2 cells. The cultured cells were incubated with Au^{3+} in DMEM medium for 1 h (**a**-**h**) and then incubated (**a**-**d**) without or (**e**-**h**) with **RHS** (20 μM) for 1 h at 37 °C. (**a**, **e**) bright-field images; (b, f) fluorescence images of nuclei counterstained with Hoechst 33,342; (**c**, **g**) fluorescence images; (**d**) merged images of (**b**-**c**) and (**h**) merged images of (**f**-**g**), respectively

plausible reaction mechanism was therefore proposed as shown Scheme 2. Upon the binding of Au^{3+}, the ring opening process was induced, followed by a 5-*exo-trig* ring closure of *N*-hydroxysemicarbazide to form 1,3,4-oxadiazole-2-one unit [44]. Notably, the *N*-arylsemicarbazide rhodamine hydrazide analog was also sensitive to Au^{3+} but led to the hydrolysis reaction [44] not the cyclization product.

Confocal Bioimaging

To further demonstrate its biological applications of **RHS** as a highly selective probe for Au^{3+}, it was applied in cultured HepG2 cells to monitor Au^{3+} (Fig. 5). HepG2 cells were washed with Dulbecco's phosphate-buffered saline buffer (DPBS, pH 7.4), and fixed by using MeOH for 20 min at −20 °C. Subsequently, the cells were treated with $HAuCl_4$ (200 μM) for 1 h and the excess Au^{3+} was removed before incubating with **RHS** (20 μM) at 37 °C for 1 h. The treated cells were stained with Hoechst 33342 nuclear staining dye (20 μM) and the fluorescence imaging was observed by excitation at 515 nm. Bright-field images indicated the cell morphology was not damaged. Cells incubated with both **RHS** and Au^{3+} exhibited a distinctive fluorescence emission, whereas cells treated with only **RHS** remained non-emissive.

Conclusions

In summary, a new rhodamine *N*-hydroxysemicarbazide **RHS** as the Au^{3+}-sensitive fluorescent chemodosimeter was developed. The fluorescent probe is highly selective to Au^{3+} with the LOD value of 0.5 μM (98 ppb) based on a 1:1 binding ratio in aqueous EtOH. The irreversible sensing mechanism of **RHS** occurred via the ring-opening spirolactam and a subsequent intramolecular 5-*exo-trig* cyclization to form the 1,3,4-oxdiazole-2-one fluorescent product. The confocal fluorescence bioimaging of **RHS** in monitoring Au^{3+} was successfully demonstrated in cultured HepG2 cells.

Supplementary Information The online version contains supplementary material available at https://doi.org/10.1007/s10895-021-02725-0.

Acknowledgements The authors acknowledge Suan Sunandha Rajabhat University, Center for Innovation in Chemistry (PERCH-CIC) and Office of National Higher Education Science Research and Innovation Policy Council (PMU-C) for financial support.

Author Contributions All authors contributed to the study conception and design. Material preparation, data collection and analysis were performed by C. Pitsanuwong, J. Boonwan, S. Chomngam, K. Wechakorn, P. Kanjanasirirat, and Y. Pewkliang. The first draft of the manuscript was written by C. Pitsanuwong and S. Chomngam. All authors commented on previous versions of the manuscript, read and approved the final manuscript.

Funding Suan Sunandha Rajabhat University, Center for Innovation in Chemistry (PERCH-CIC) and Office of National Higher Education Science Research and Innovation Policy Council (PMU-C).

Data Availability All the data and materials from this manuscript will be made available on request.

Declarations

Ethics Declarations Not applicable.

Conflict of Interest Authors declare that they have no conflict of interest.

References

1. Bertelsen S, Jørgensen KA (2009) Organocatalysis - After the gold rush. Chem Soc Rev 38(8):2178–2189. https://doi.org/10.1039/b903816g
2. Liu G, Li G, Song H (2009) Direct synthesis of methyl propionate from n-propyl alcohol and methanol using gold catalysts. Catal Lett 128(3–4):493–501. https://doi.org/10.1007/s10562-008-9782-0
3. Sardar R, Funston AM, Mulvaney P, Murray RW (2009) Gold nanoparticles: Past, present, and future. Langmuir 25(24):13840–13851. https://doi.org/10.1021/la9019475
4. Yamamoto Y, Gridnev ID, Patil NT, Jin T (2009) Alkyne activation with Brønsted acids, iodine, or gold complexes, and its fate leading to synthetic application. ChemComm (34):5075–5087. https://doi.org/10.1039/b909978f
5. Arcadi A (2008) Alternative synthetic methods through new developments in catalysis by gold. Chem Rev 108(8):3266–3325. https://doi.org/10.1021/cr068435d
6. Hashmi ASK, Rudolph M (2008) Gold catalysis in total synthesis. Chem Soc Rev 37(9):1766–1775. https://doi.org/10.1039/b615629k
7. Jiménez-Núñez E, Echavarren AM (2008) Gold-catalyzed cycloisomerizations of enynes: A mechanistic perspective. Chem Rev 108(8):3326–3350. https://doi.org/10.1021/cr0684319
8. Li Z, Brouwer C, He C (2008) Gold-catalyzed organic transformations. Chem Rev 108(8):3239–3265. https://doi.org/10.1021/cr0684341
9. Sannella AR, Casini A, Gabbiani C, Messori L, Bilia AR, Vincieri FF, Majori G, Severini C (2008) New uses for old drugs. Auranofin, a clinically established antiarthritic metallodrug, exhibits potent antimalarial effects in vitro: Mechanistic and pharmacological implications. FEBS Lett 582(6):844–847. https://doi.org/10.1016/j.febslet.2008.02.028
10. Nobili S, Mini E, Landini I, Gabbiani C, Casini A, Messori L (2010) Gold compounds as anticancer agents: Chemistry, cellular pharmacology, and preclinical studies. Med Res Rev 30(3):550–580. https://doi.org/10.1002/med.20168
11. Berners-Price SJ, Filipovska A (2011) Gold compounds as therapeutic agents for human diseases. Metallomics 3(9):863–873. https://doi.org/10.1039/c1mt00062d
12. Ghosh P, Han G, De M, Kim CK, Rotello VM (2008) Gold nanoparticles in delivery applications. Adv Drug Deliv Rev 60(11):1307–1315. https://doi.org/10.1016/j.addr.2008.03.016
13. Boisselier E, Astruc D (2009) Gold nanoparticles in nanomedicine: Preparations, imaging, diagnostics, therapies and toxicity. Chem Soc Rev 38(6):1759–1782. https://doi.org/10.1039/b806051g

14. Giljohann DA, Seferos DS, Daniel WL, Massich MD, Patel PC, Mirkin CA (2010) Gold nanoparticles for biology and medicine. Angew Chem Int Ed 49(19):3280–3294. https://doi.org/10.1002/anie.200904359
15. Dykman L, Khlebtsov N (2012) Gold nanoparticles in biomedical applications: Recent advances and perspectives. Chem Soc Rev 41(6):2256–2282. https://doi.org/10.1039/c1cs15166e
16. Connor EE, Mwamuka J, Gole A, Murphy CJ, Wyatt MD (2005) Gold nanoparticles are taken up by human cells but do not cause acute cytotoxicity. Small 1(3):325–327. https://doi.org/10.1002/smll.200400093
17. Pedersen DS, Locht LJ, Tran TP, Markholt S, Rungby J, Larsen A (2014) Toxicological aspects of injectable gold-hyaluronan combination as a treatment for neuroinflammation. Histol Histopathol 29(4):447–456
18. Kocúrová L, Balogh IS, Škrlíková J, Posta J, Andruch V (2010) A novel approach in dispersive liquid-liquid microextraction based on the use of an auxiliary solvent for adjustment of density: UV-VIS spectrophotometric and graphite furnace atomic absorption spectrometric determination of gold based on ion pair formation. Talanta 82(5):1958–1964. https://doi.org/10.1016/j.talanta.2010.08.028
19. Young Choi J, Kim GH, Guo Z, Yeon Lee H, Swamy KMK, Pai J, Shin S, Shin I, Yoon J (2013) Highly selective ratiometric fluorescent probe for Au^{3+} and its application to bioimaging. Biosens Bioelectron 49:438–441. https://doi.org/10.1016/j.bios.2013.05.033
20. Song F, Ning H, She H, Wang J, Peng X (2014) A turn-on fluorescent probe for Au^{3+} based on rodamine derivative and its bioimaging application. Sci China Chem 57(7):1043–1047. https://doi.org/10.1007/s11426-014-5107-x
21. Üçüncü M, Emrullahoğlu M (2014) A BODIPY-based reactive probe for the detection of Au(iii) species and its application to cell imaging. Chem Commun 50(44):5884–5886. https://doi.org/10.1039/c4cc01958j
22. Memon S, Bhatti AA, Bhatti AA, Ocak Ü, Ocak M (2015) Calix[4]arene based highly efficient fluorescent sensor for Au^{3+} and I. J Fluoresc 25(5):1507–1515. https://doi.org/10.1007/s10895-015-1642-x
23. Wechakorn K, Prabpai S, Suksen K, Piyachaturawat P, Kongsaeree P (2016) Rhodol-based fluorescent probe for Au^{3+} detection and its application in bioimaging. RSC Adv 6(29):24752–24755. https://doi.org/10.1039/c6ra02342h
24. Liu Y, Song F, Guo S (2006) Cleavage of a carbon-carbon triple bond via gold-catalyzed cascade cyclization/oxidative cleavage reactions of (2)-enynols with molecular oxygen. J Am Chem Soc 128(35):11332–11333. https://doi.org/10.1021/ja062610q
25. Lee JH, Park J, Lah MS, Chin J, Hong JI (2007) High-affinity pyrophosphate receptor by a synergistic effect between metal coordination and hydrogen bonding in water. Org Lett 9(19):3729–3731. https://doi.org/10.1021/ol071306e
26. Zhang JF, Zhou Y, Yoon J, Kim JS (2011) Recent progress in fluorescent and colorimetric chemosensors for detection of precious metal ions (silver, gold and platinum ions). Chem Soc Rev 40(7):3416–3429. https://doi.org/10.1039/c1cs15028f
27. Duman N, Ersoy-Evans S, Karadağ Ö, Aşçioğlu S, Şener B, Kiraz S, Şahin S (2014) Screening for latent tuberculosis infection in psoriasis and psoriatic arthritis patients in a tuberculosis-endemic country: A comparison of the QuantiFERON®-TB Gold In-Tube test and tuberculin skin test. Int J Dermatol 53(10):1286–1292
28. Seo H, Jun ME, Ranganathan K, Lee KH, Kim KT, Lim W, Rhee YM, Ahn KH (2014) Ground-state elevation approach to suppress side reactions in gold-sensing systems based on alkyne activation. Org Lett 16(5):1374–1377. https://doi.org/10.1021/ol5001389
29. Lee H, Park HY, Jeon K, Jeong BH, Hwang JW, Lee J, Cha HS, Koh EM, Kang ES, Koh WJ (2015) PLoS One 10:1
30. Srisuratsiri P, Kanjanasirirat P, Chairongdua A, Kongsaeree P (2017) Reversible rhodamine-alkyne Au^{3+}-selective chemosensor and its bioimaging application. Tet Lett 58(32):3194–3199. https://doi.org/10.1016/j.tetlet.2017.07.014
31. Li Z, Xu Y, Fu J, Zhu H, Qian Y (2018) Monitoring of Au(III) species in plants using a selective fluorescent probe. ChemComm 54(8):888–891. https://doi.org/10.1039/c7cc08333e
32. Egorova OA, Seo H, Chatterjee A, Ahn KH (2010) Reaction-based fluorescent sensing of Au(I)/Au(III) species: Mechanistic implications on vinylgold intermediates. Org Lett 12(3):401–403
33. Saleem M, Lee K-H (2014) Selective fluorescence detection of Cu^{2+} in aqueous solution and living cells. J Lumin 145:843–848. https://doi.org/10.1016/j.jlumin.2013.08.044
34. Yang J-p, Fei L, Jing C, Yang J-d (2015) Sensing and magnetic removal of Hg(II) using core-shell structured nanocomposite grafted with fluorescence "Off-On" probe. Microporous Mesoporous Mater 202:175–182. https://doi.org/10.1016/j.micromeso.2014.09.054
35. Zhao Y-C, Chen C, Chen B, Wang P-Y, Wu Z-B, Li H, Song B-A, Yang S (2017) Tunable fluorescent probes for selective detection of copper(II) and sulfide with completely different modes. Sens Actuators B Chem 241:168–173. https://doi.org/10.1016/j.snb.2016.10.071
36. Hu JH, Long C, Fu QQ, Ni PW, Yin ZY (2019) A novel highly selective colorimetric and "turn-on" fluorimetric chemosensor for detecting Hg^{2+} based on Rhodamine B hydrazide derivatives in aqueous media. J Photochem Photobiol A 379:105–111. https://doi.org/10.1016/j.jphotochem.2019.04.031
37. Long C, Hu JH, Fu QQ, Ni PW (2019) A new colorimetric and fluorescent probe based on Rhodamine B hydrazone derivatives for cyanide and Cu^{2+} in aqueous media and its application in real life. Spectrochim Acta A Mol Biomol Spectrosc 219:297–306. https://doi.org/10.1016/j.saa.2019.04.052
38. Deepa A, Srinivasadesikan V, Lee SL, Padmini V (2020) Highly selective and sensitive colorimetric and Fluorimetric sensor for Cu2+. J Fluoresc 30(1):3–10. https://doi.org/10.1007/s10895-019-02450-9
39. Dujols V, Ford F, Czarnik AW (1997) A long-wavelength fluorescent chemodosimeter selective for Cu(II) ion in water. J Am Chem Soc 119(31):7386–7387. https://doi.org/10.1021/ja971221g
40. Young JR, DeVita RJ (1998) Novel synthesis of Oxadiazoles via palladium catalysis. Tet Lett 39(23):3931–3934. https://doi.org/10.1016/S0040-4039(98)00719-9
41. Aljaar N, Conrad J, Beifuss U (2013) Synthesis of 2-aryl-1,2-dihydrophthalazines via reaction of 2-(bromomethyl)benzaldehydes with arylhydrazines. J Org Chem 78(3):1045–1053. https://doi.org/10.1021/jo302491x
42. Vodela S, Mekala RVR, Danda RR, Kodhati V (2013) Design, synthesis and screening of some novel benzoxazole based 1,3,4-oxadiazoles as potential antimicrobial agents. Chin Chem Lett 24(7):625–628. https://doi.org/10.1016/j.cclet.2013.04.005
43. Brahmayya M, Dai SA, Suen SY (2015) Synthesis of 5-substituted-3H-[1,3,4]-oxadiazol-2-one derivatives: A carbon dioxide route (CDR). RSC Adv 5(80):65351–65357. https://doi.org/10.1039/c5ra08910g
44. Patel KD, Prajapati SM, Panchal SN, Patel HD (2014) Review of synthesis of 1,3,4-oxadiazole derivatives. Synth Commun 44(13):1859–1875. https://doi.org/10.1080/00397911.2013.879901